Sympathetic Tripping Problem Analysis and Solutions

Jeff Roberts
Schweitzer Engineering Laboratories, Inc.

Terrence L. Stulo
Nevada Power Company

Andres Reyes
Omicron Electronics Corp. USA

Revised edition released May 2002

Previously presented at the
12th Annual CEPSI Exhibition, November 1998,
and 52nd Annual Georgia Tech Protective Relaying Conference, May 1998

Originally presented at the
24th Annual Western Protective Relay Conference, October 1997

SYMPATHETIC TRIPPING PROBLEM ANALYSIS AND SOLUTIONS

Jeff Roberts
Schweitzer Engineering Laboratories, Inc.
Pullman, WA USA

Terrence L. Stulo
Nevada Power Company
Las Vegas, NV USA

Andres Reyes
Omicron Electronics Corp. USA
Houston, TX USA

INTRODUCTION

Sympathetic trips are undesirable relay operations for unbalanced- or high-load conditions which occur during or immediately following out-of-section faults. The root cause of the sympathetic trip problem is the type and connection of loads served by distribution feeders. There are two classifications of sympathetic trips: those which occur due to delayed voltage recovery conditions, and those which occur due to the load unbalance during an out-of-section fault.

Several other technical papers discuss how to avoid sympathetic tripping of radial feeders: [3], [4], and [5]. These papers described the system operating conditions preceding sympathetic trip occurrences, the resulting power system disruption, and the costly capital expenditures thought necessary to avoid the tripping problem. One common sympathetic trip solution offered in these papers is to permanently raise phase and ground overcurrent element pickup thresholds. This solution unnecessarily penalizes fault detection sensitivity.

This paper describes two simple relay-based solutions which give the necessary sympathetic trip security and maintain the desired fault detection sensitivity. This paper also includes system examples which illustrate how to include load impedances in symmetrical component network connections.

THE DELAYED VOLTAGE RECOVERY SYMPATHETIC TRIPPING PROBLEM

Delayed voltage recovery conditions (i.e., extended duration voltage sags) are commonly initiated by a fault on adjacent lines of the same voltage level or on higher voltage source lines. The delayed voltage recovery problem is a result of the type of connected load. The culprit loads are large blocks of low-inertia induction motors that lose speed rapidly during a fault-caused voltage sag. Single-phase residential air conditioners are a common application for these motors. Compounding their already easy-to-stall characteristics, these same motors must also work against a high refrigerant gas pressure held in the compressor itself. As these motors stall, they draw more current as the effective motor impedance decreases. Appendix A shows the printout of a mathematical program useful for characterizing motor impedance as a function of slip (where slip is defined as the difference in actual motor speed and ideal synchronous speed). Given that there could be many air conditioners served by a single feeder, the increase in feeder load current for the affected phase(s) can be appreciable. It is this large block of motor current draw which leads to the troublesome sympathetic tripping by distribution feeder protective overcurrent relays.

Delayed Voltage Recovery Occurrences Which Resulted in Sympathetic Trips

Sympathetic tripping occurrences due to delayed voltage recovery are not rare. The following list shows some recorded delayed voltage recovery sympathetic tripping cases:

- Southern California Edison (SCE), Los Angeles Basin area of California: 10 incidents spanning 1990 - 1992. One event affected a 1000 square mile area [3].
- Sacramento Municipal Utility District (SMUD), Sacramento, California: August 1990, twelve 12.47 kV breakers suspected of tripping due to sympathetic tripping [3].
- Central Power and Light (CP&L), Corpus Christi, Texas: 89 sympathetic tripping events from September 1, 1990 to March 1, 1993 [4].

We suspect that many other sympathetic tripping instances have occurred but remain unexplained. This is simply because older protective relays do not record fault information and fault recorders are not commonplace at the distribution feeder level.

Delayed voltage recovery sympathetic tripping instances are likely to increase as line loading and the amount of single-phase, low-inertia air compressor motor loads increase.

Background of The New Delayed Voltage Recovery Sympathetic Trip Solutions

The sympathetic trip solutions offered next are both cost effective and simple. Both solutions are easily implemented in a protective relay or similar type device that measures three voltages and three currents and calculates symmetrical component voltages and currents from these phase quantities.

Adjacent Feeder Faults Induce Sympathetic Feeder Trips

Let us examine the delayed voltage recovery problem for a ground fault on a parallel distribution line.

Figure 2 shows the sequence connection diagram for the A-phase-ground fault on Line 2 shown in the system single-line diagram of Figure 1. This single-line-ground fault is located at m = 0.5 where m is the per-unit line length.

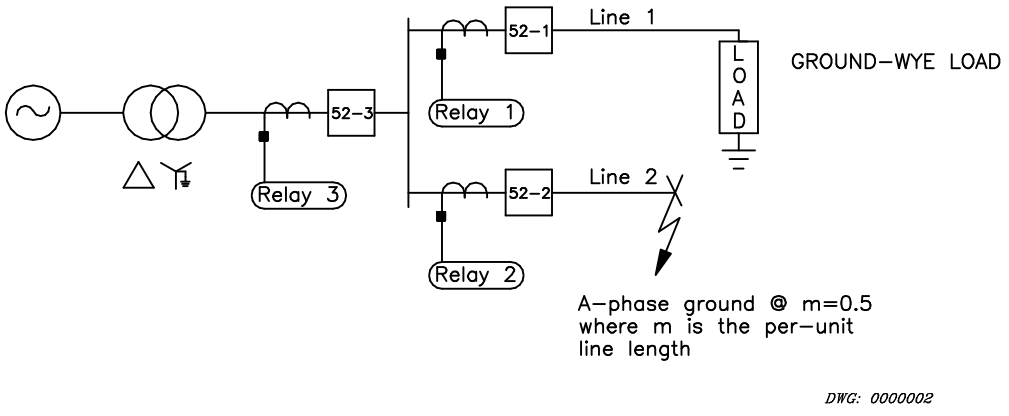

Figure 1: Single-Line Diagram for an Adjacent Feeder Fault on a Radial System

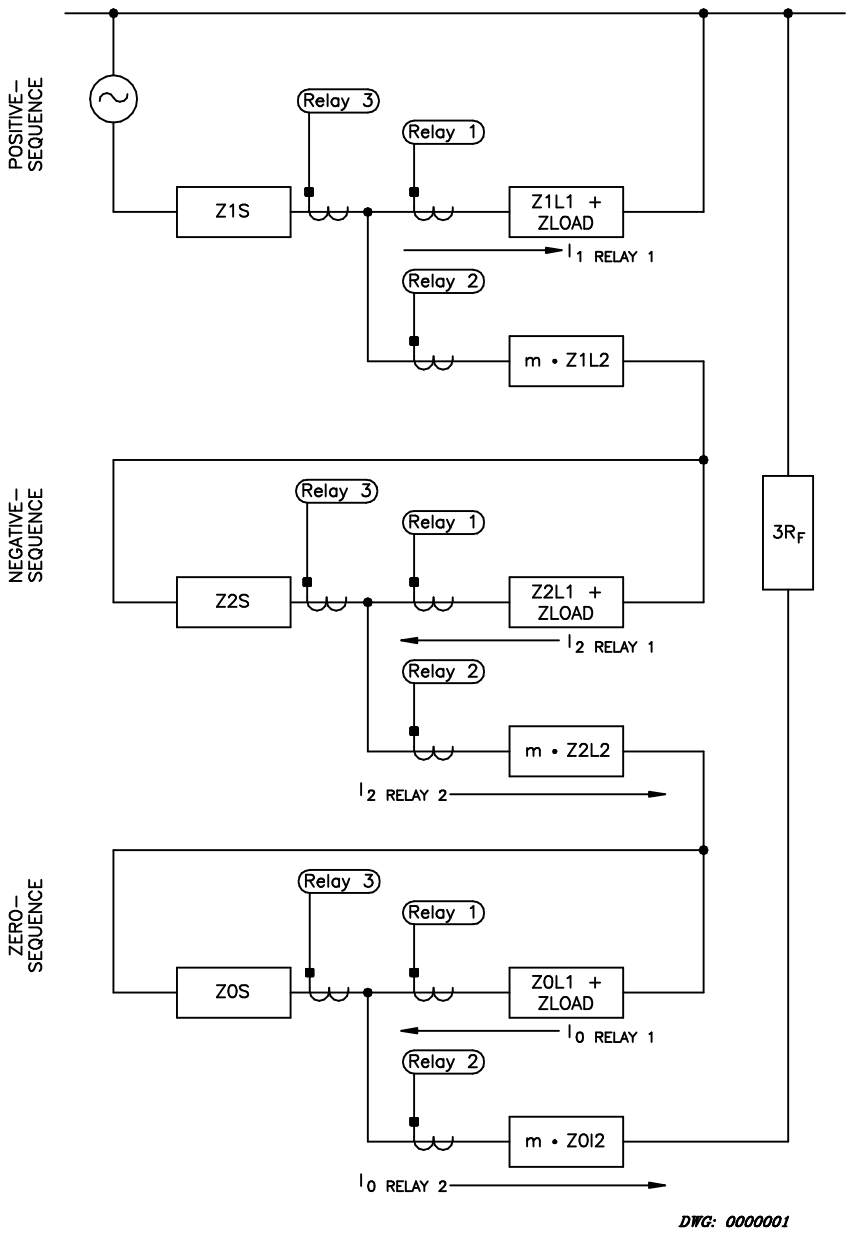

Figure 2: Sequence Connection Diagram of a Ground Fault on Adjacent Feeder for a Radial System

For any ground fault on Line 2, the desired actions of the three relays shown in Figure 1 are listed below:

1. Relay 2 trips Breaker 52-2.
2. Relay 3 senses the ground fault but does not trip Breaker 52-3 unless Breaker 52-2 fails.
3. Relay 1 does not trip (because the line is not faulted), Breaker 52-1 remains closed, and the load served by Line 1 remains energized (assuming Breaker 52-3 remains closed).

In this example, assume Line 1 has significant single-phase, low-inertia motor loads connected at the end of the feeder (such as you might see if there was a large block of newer residential housing load located at the end of a feeder).

The system parameters in secondary ohms for the example system of Figure 1 are

Positive-, Zero-Sequence Source Impedance:	$Z_{1S,\,0S}$	= 1 Ω ∠84.3°
Positive-Sequence Line Impedance:	$Z_{1L1,\,1L2}$	= 8.54 Ω ∠69°
Zero-Sequence Line Impedance:	$Z_{0L1,\,0L2}$	= 25.63 Ω ∠69°
Per-Phase Load Impedance (includes motors)	Z_{LOAD}	= 6.43 Ω ∠41.3°

The value of load impedance listed is accurate with the motor load very near synchronous speed: slip = 0.02. The motor load is modeled as a single, low-inertia motor to illustrate a worst-case scenario where all motors stall simultaneously. For slip = 0.02, the motor load impedance equals 5.1 Ω secondary. As the motor load speed decreases, the slip increases and the motor impedance decreases.

With Line 2 faulted, the A-phase distribution voltage magnitude depresses. This voltage depression tends to stall the single-phase motor load connected to A-phase on Line 1. Figure 3 shows the $|3I_0|$ and $|3I_2|$ currents measured by Relay 1 during and after the Line 2 fault.

Both $|3I_0|$ and $|3I_2|$ currents flow in Line 1 for a fault on Line 2. From Figure 2, notice that the direction of $3I_0$ and $3I_2$ current flow is into bus as measured by Relay 1. This is the same current flow direction as that of a reverse direction fault.

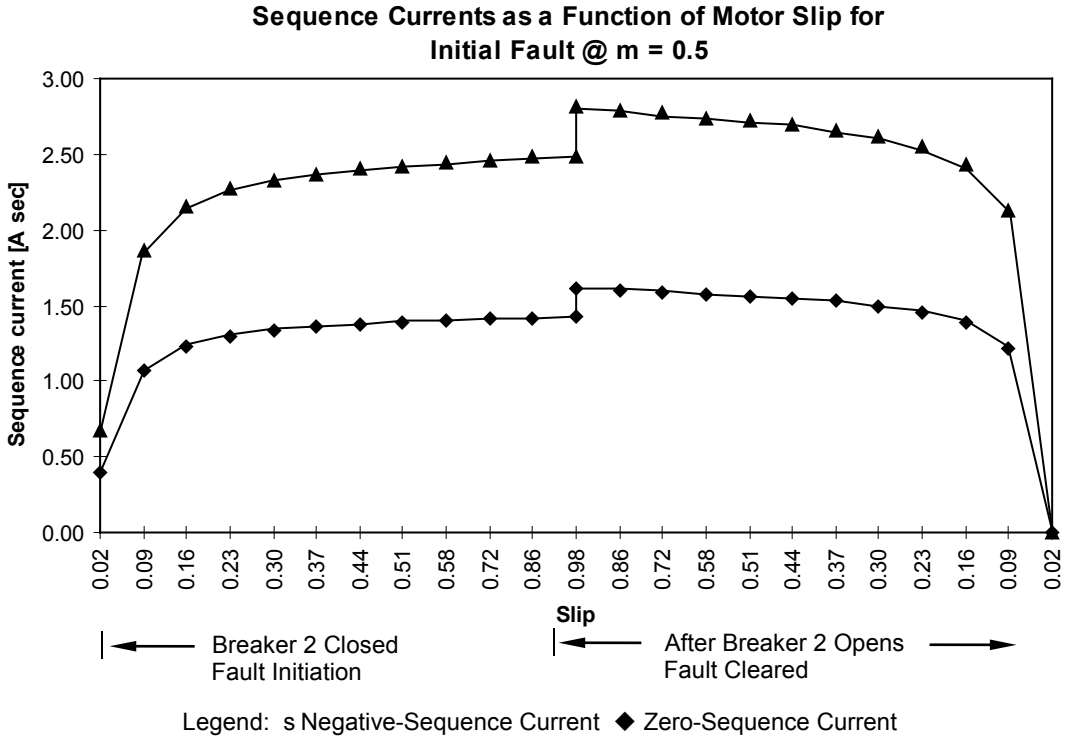

Figure 3: Line 1 Motor Slip Changes the $|3I_2|$ and $|3I_0|$ Currents Measured by Relay 1 During and After the Line 2 A-Phase Feeder Fault

From Figure 3, notice that the $|3I_2|$ and $|3I_0|$ currents measured by Relay 1 increase as the Line 1 motor load slip increases. If the nondirectional ground overcurrent protection for Relay 1 is low-set, this protection could operate undesirably. For example, if the nondirectional residual time-overcurrent element for Relay 1 has a pickup of 1 A, this element should pick up for a fault on Line 2. This element remains picked up until the motor loads on all three phases become balanced (the motor load connected to A-phase regains synchronous speed).

Real World Example #1: Adjacent 12.24 kV Feeder Fault

On August 9, 1997, Nevada Power Company (NPC) experienced a BC-ground fault on Feeder 1215 (see Figure 4). The suspected cause of this fault was lightning. Protective relays for Feeders 1215 and 1210 triggered event reports for this same fault. The Feeder 1215 relay correctly generated a trip output initiated by its nondirectional phase time-overcurrent element. Figure 5 and Figure 6 show the phase-voltage and current magnitudes. Figure 7 and Figure 8 show the sequence voltages and currents measured by the protective relays for Feeders 1210 and 1215.

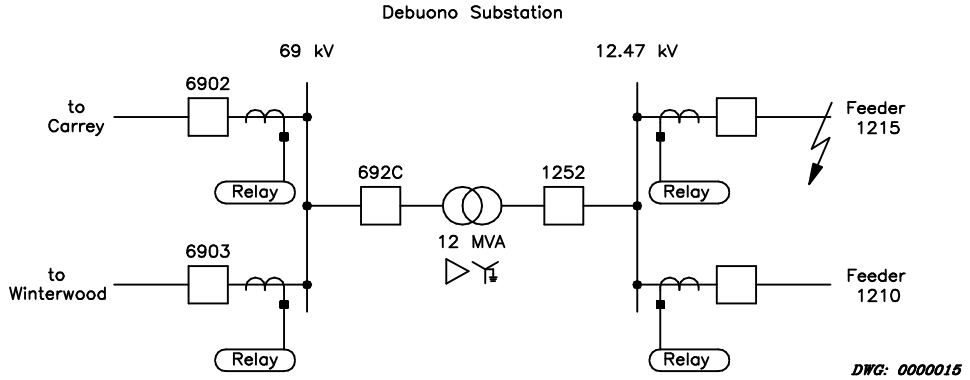

Figure 4: System Single-Line Diagram for NPC Real World Example

From Figure 6, notice that the fault type begins as BC-ground near Cycle 4 and evolves to a three-phase fault in Cycle 8. The protection system for Feeder 1215 cleared this fault at Cycle 29: relay trip time of 26 cycles, breaker operate time of 3 cycles.

While Feeder 1210 is not faulted, it does experience a significant increase in both phase and sequence currents during and after the fault on the adjacent feeder. From Figure 5, we see that the highest phase current for Feeder 1210 exceeded the phase time-overcurrent element pickup of 3.0 A secondary near Cycle 29, immediately after the fault on Feeder 1215 clears.

From Figure 7, notice that $3I_0$ current on Feeder 1210 exceeded the ground time-overcurrent element pickup of 1.0 A secondary near Cycle 4 and again near Cycle 23. As we discussed earlier, these high currents on Feeder 1210 can exist for an extended time after the adjacent feeder clears the fault. Feeder 1210 did not trip because of the correct action of its sympathetic trip logic. We discuss this logic later in this paper.

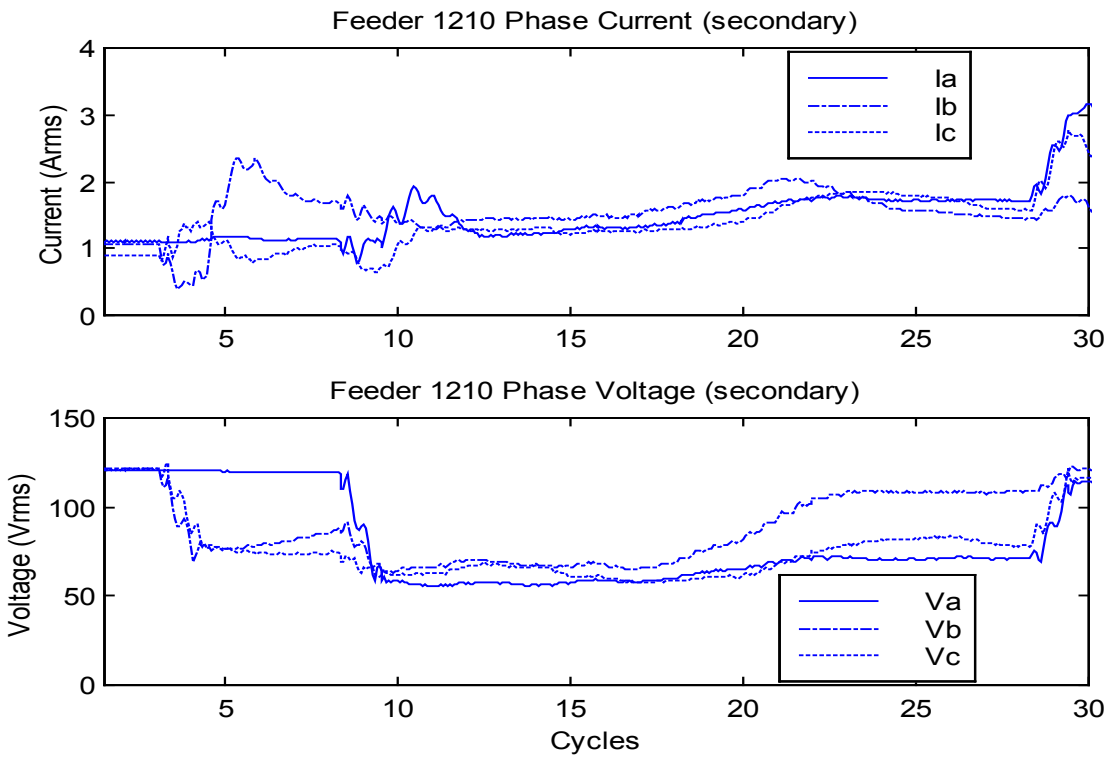

Figure 5: Phase Voltages and Currents Measured by the Feeder 1210 Relay

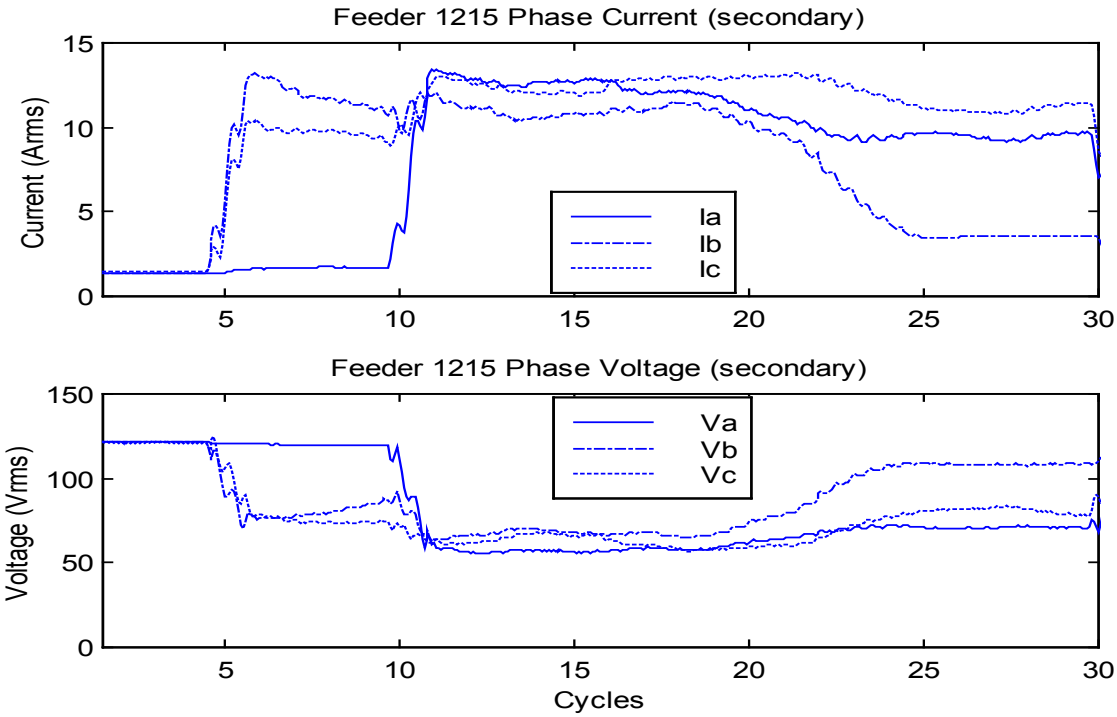

Figure 6: Phase Voltages and Currents Measured by the Feeder 1215 Relay

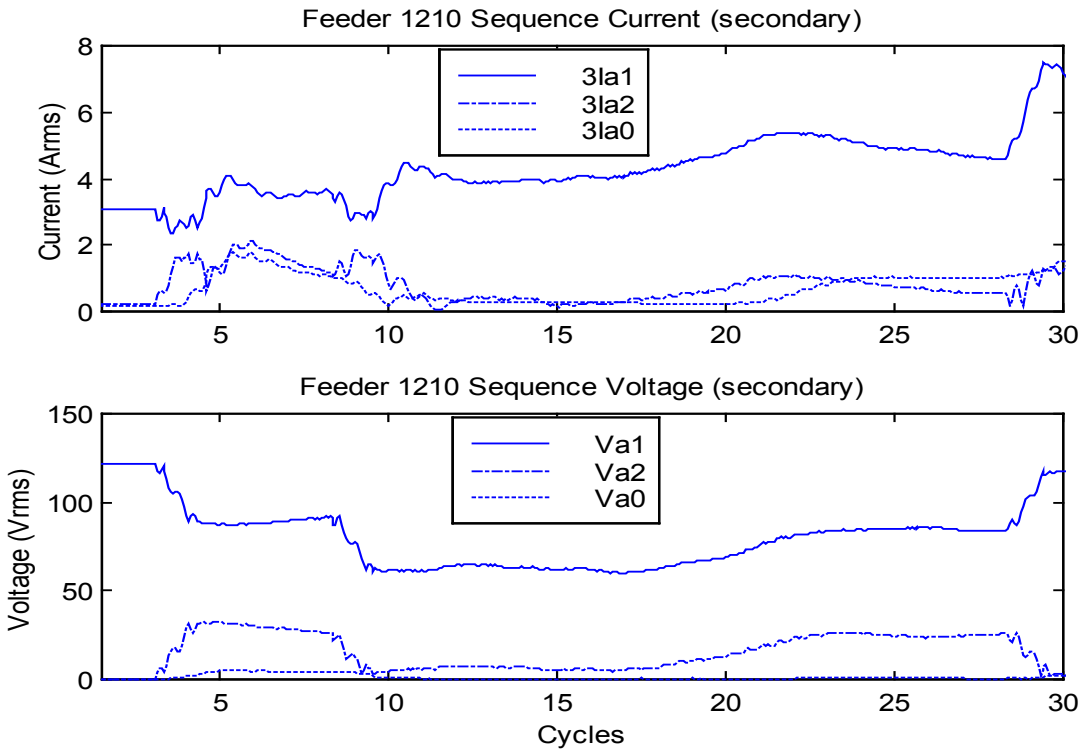

Figure 7: Sequence Voltages and Currents Measured by the Feeder 1210 Relay

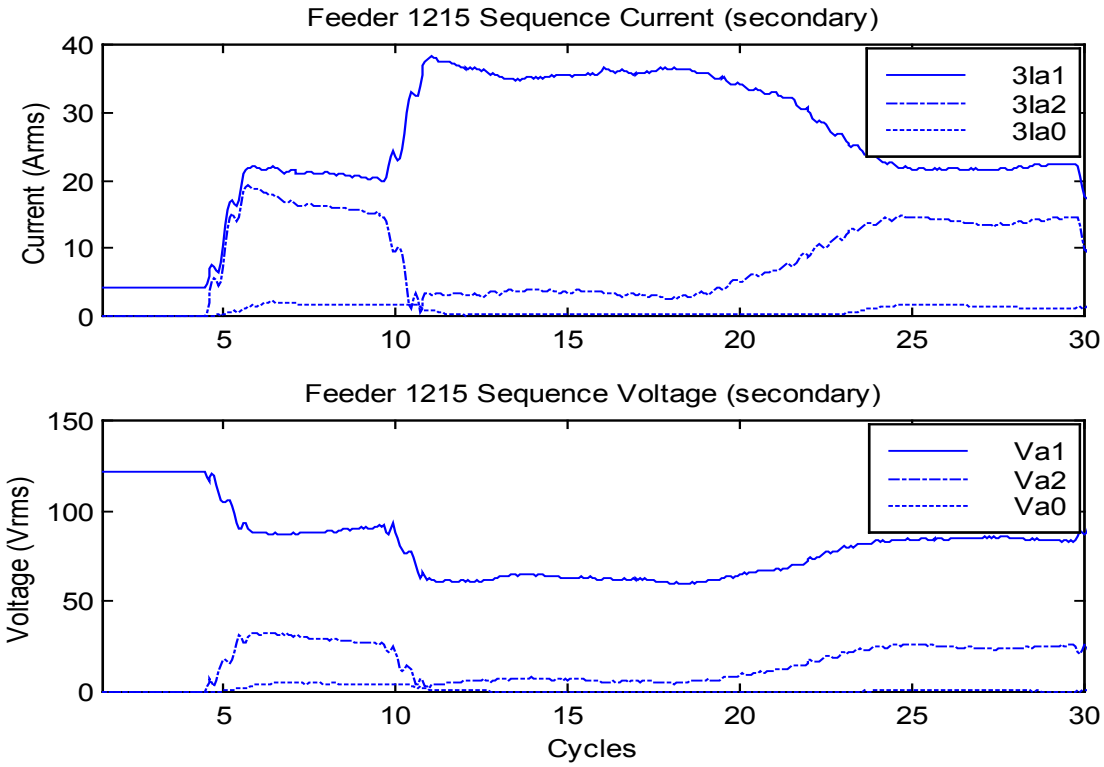

Figure 8: Sequence Voltages and Currents Measured by the Feeder 1215 Relay

Transmission Line Faults Also Induce Sympathetic Tripping of Feeder Relays

Any fault on a high-voltage power line reduces the phase voltage on many distribution feeders. Let us next examine the sequence connection diagram for a ground fault on a high-voltage power line (see Figure 9).

Figure 10 shows the sequence network diagram for the A-phase-ground fault on Line 2 as depicted in the system single-line diagram in Figure 9. From Figure 9 notice that the distribution load is on the low-voltage side of the delta-wye-grounded power transformer. Relays 8 and 9 should not trip for the fault shown because neither Line 4 or 5 is faulted.

During the transmission line fault shown in Figure 9, the A-phase-voltage magnitude depresses at all relay terminals. How much the motor terminal voltages on Lines 4 and 5 depress depends on proximity of the motor terminal to the fault. It is during this reduced voltage that the motor loads connected to Lines 4 and 5 begin to stall. When Breakers 52-3 and 52-4 open to clear the ground fault, the A- and C-phase voltages for Lines 4 and 5 recover slightly. (Later we discuss why two distribution feeder voltages depress for this high-voltage ground fault). However, these phase voltages can remain less than nominal due to the increased current drawn by the motor loads (this is due to the increase in line voltage drop).

Referring again to Figure 10, notice that $3I_2$ current flows in Lines 4 and 5 during the fault on Line 2. The direction of this $3I_2$ current flow is into the bus as measured by Relays 8 and 9. This is the direction of current flow associated with a reverse direction fault.

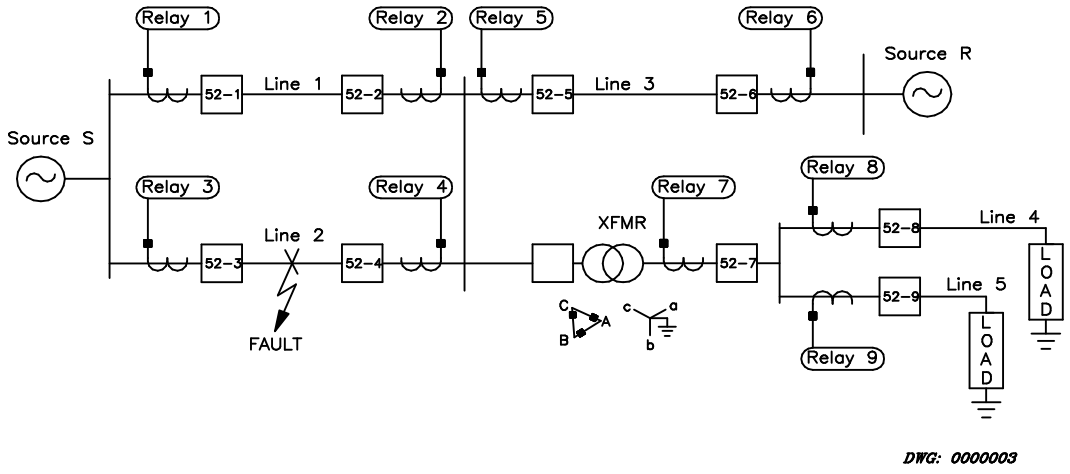

Figure 9: System Single-Line Diagram for High Voltage A-Phase-Ground Fault

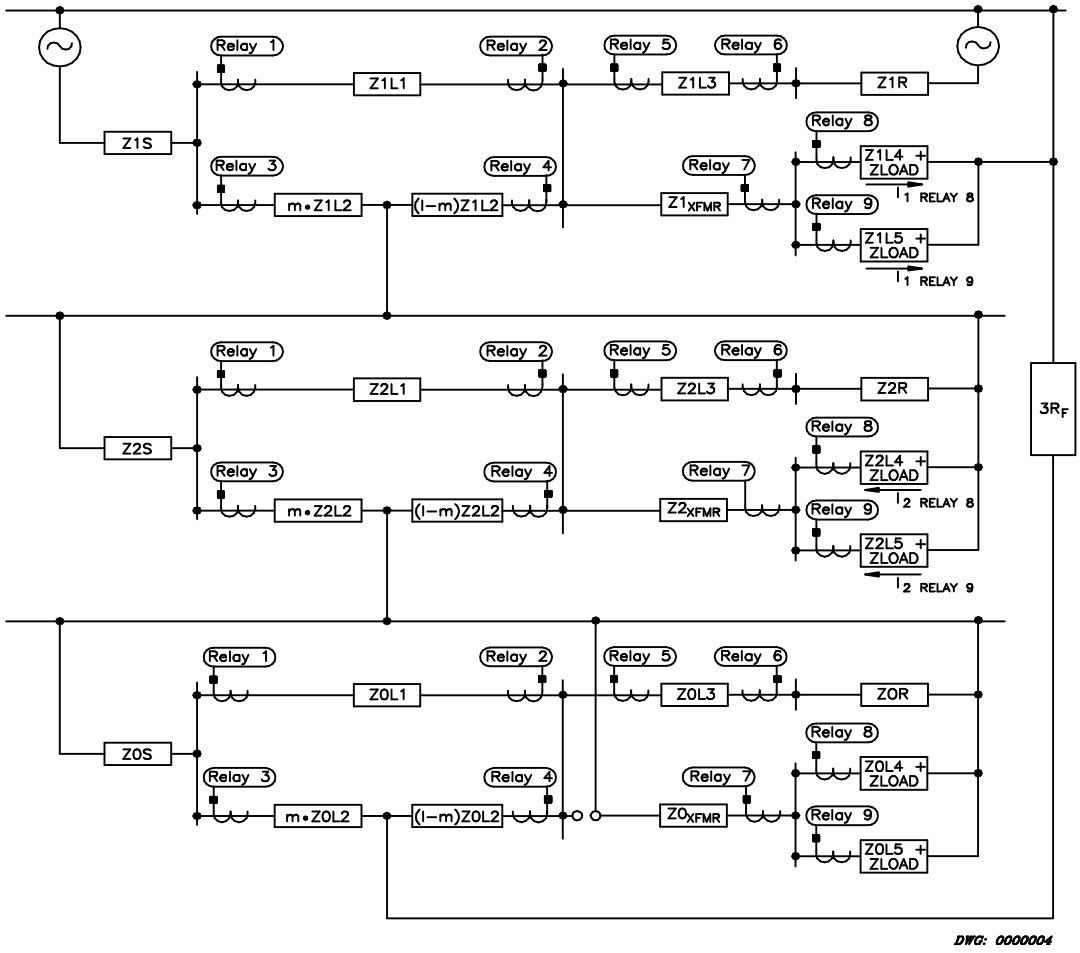

Figure 10: Sequence Connection Diagram for High Voltage A-Phase-Ground Fault

Real World Example #2: 69 kV Transmission Line A-Phase-Ground Fault

Approximately 15 minutes after the BC-ground fault on Feeder 1215, one of the 69 kV transmission lines serving Feeders 1210 and 1215 experienced an A-phase-ground fault. Again, the suspected cause of the fault was lightning. This fault later evolved to an AB-ground fault just prior to the 69 kV breaker operation. The protective relays for the 69 kV line terminal and Feeders 1215 and 1210 triggered event reports for this same fault. Again, neither feeder relay issued a trip because of the correct action of their sympathetic trip logic.

Figure 11 and Figure 13 show the phase voltage and current magnitudes measured by the feeder relays before, during, and immediately after the 69 kV fault. Figure 12 and Figure 14 show the sequence voltages and currents measured by the feeder relays for this same 69 kV fault.

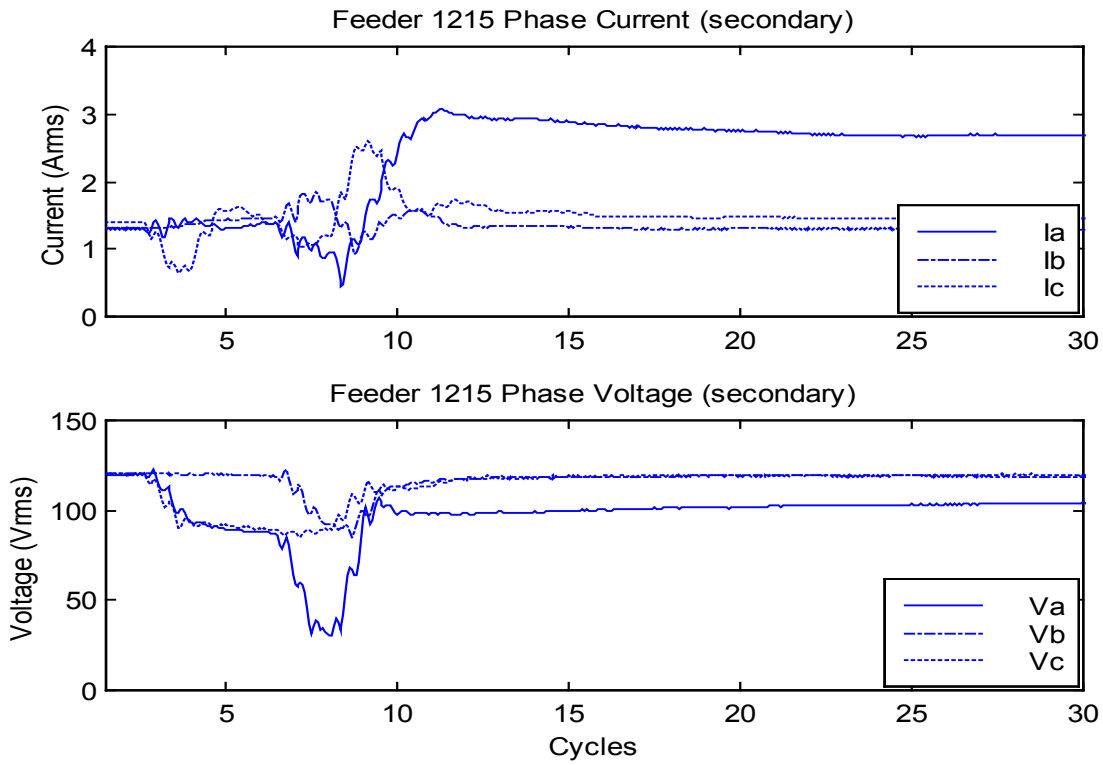

Figure 11: Phase Voltages and Currents Measured by the Feeder 1215 Relay

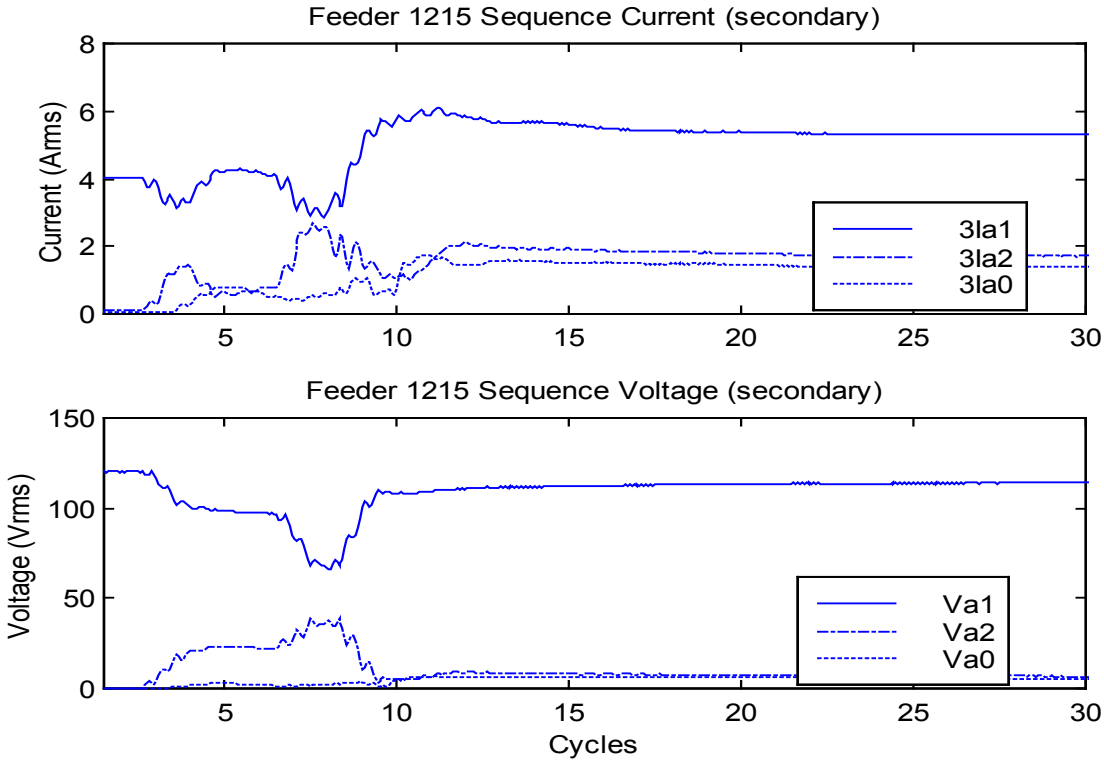

Figure 12: Sequence Voltages and Currents Measured by the Feeder 1215 Relay

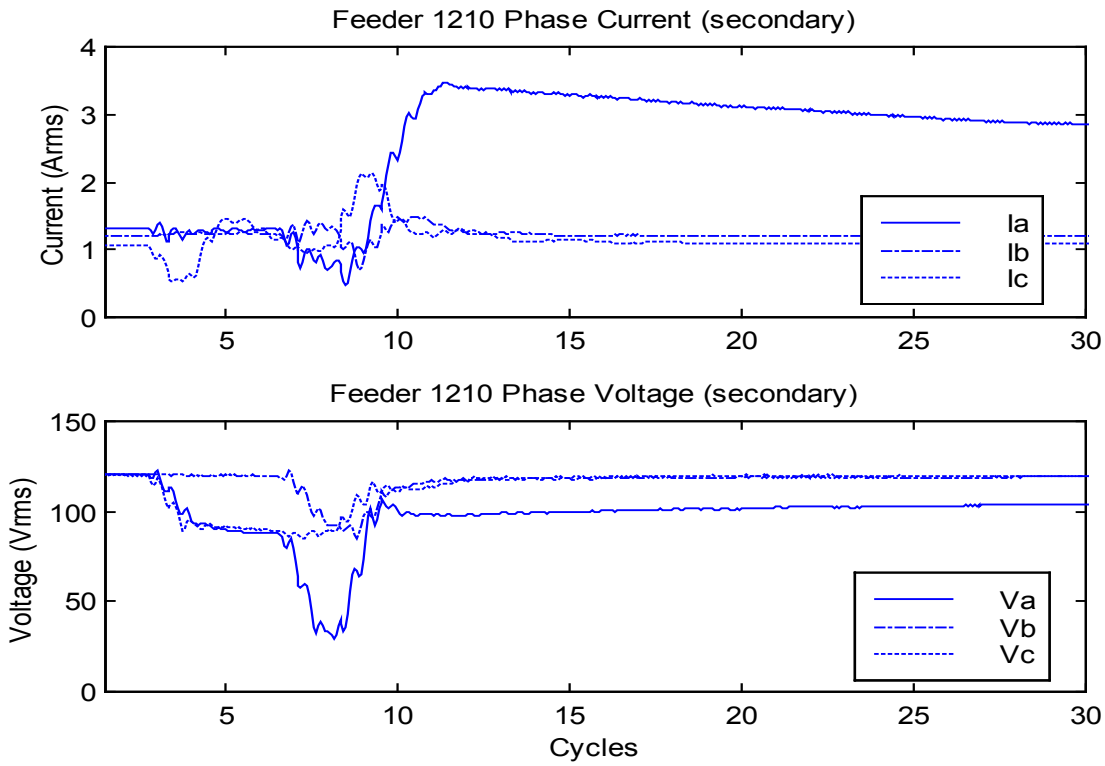

Figure 13: Phase Voltages and Currents Measured by the Feeder 1210 Relay

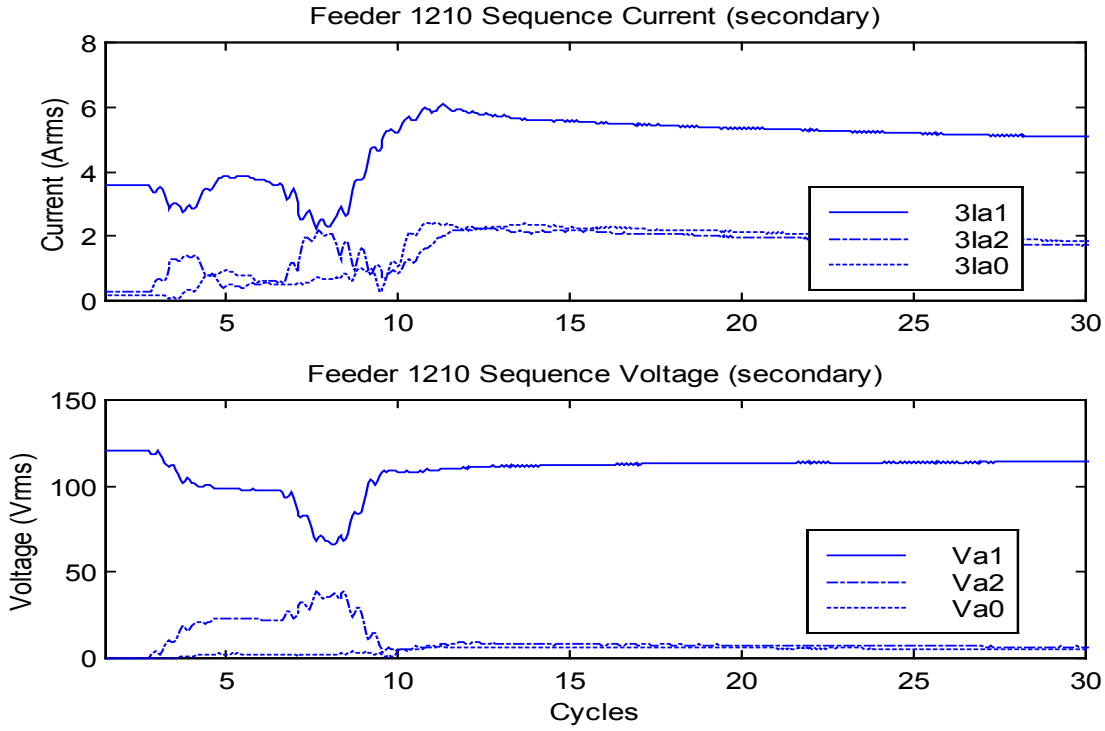

Figure 14: Sequence Voltages and Currents Measured by the Feeder 1210 Relay

From Figure 11 and Figure 13, notice that only the A- and C-phase distribution voltage magnitudes are initially depressed for the transmission line fault. We expect two distribution phase voltages to depress for a ground fault on the high-voltage side of a delta-wye-grounded power transformer. Also notice that near Cycle 8, all three phase-voltage magnitudes decrease when the 69 kV fault evolved to a AB-ground fault.

The phasor diagram in Figure 15 illustrates how the distribution feeder voltages depress for a bolted A-phase-ground fault on the high-voltage side of a delta-wye-grounded power transformer. Capital letter subscripts indicate transmission system voltages while lower case subscripts indicate distribution system voltages. Figure 16 shows the distribution feeder voltages measured when the high voltage A-phase-ground fault evolves to an AB-ground fault.

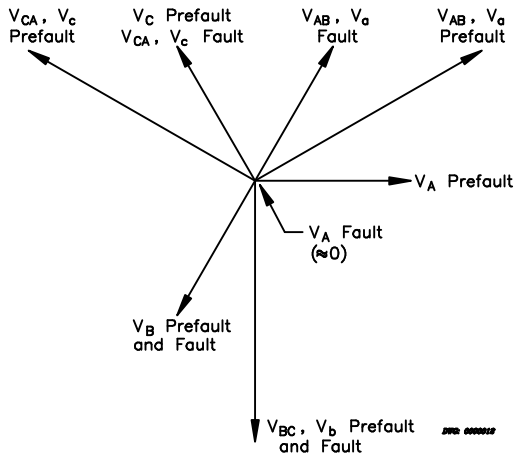

Figure 15: Feeder Relay Voltages Measured for an A-Phase-Ground Fault on the High Voltage Side of a Delta-Wye-Grounded Transformer

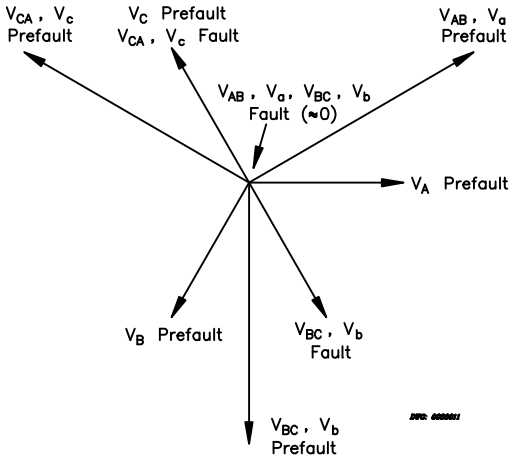

Figure 16: Feeder Relay Voltages Measured for an AB-Phase-Ground Fault on the High Voltage Side of a Delta-Wye-Grounded Transformer

From Figure 11 and Figure 13, notice the extreme decrease in the A-phase feeder voltage magnitude once the transmission line fault evolved. This large distribution voltage sag is the same as that predicted in Figure 16. Reference [3] states that "prone-to-stall motors stall for nearly all faults with a duration greater than five cycles with less than 60% nominal voltage." Because the A-phase-voltage magnitude dropped below 60% of nominal, motors connected to this phase stalled. To see the effect of these motors stalling, notice the large increase in A-phase current magnitude after the 69 kV fault cleared (see Figure 13).

The data in Figure 11 through Figure 14 show that while neither Feeder 1215 or 1210 were faulted, both experienced significant increases in phase and sequence currents during and after the fault. From Figure 11 and Figure 13, we see that the highest phase current for both feeders exceeded the phase time-overcurrent element pickup of 3.0 A secondary near Cycle 10. The protective relay for Feeder 1210 measured a slightly greater current than did the relay for Feeder 1215. This is possibly due to slightly more motor load on Feeder 1210. From Figure 12 and Figure 14, we can see that the residual current (3I0) on both feeders exceeded the ground time-overcurrent element pickup thresholds of 1.0 A for both feeders near Cycle 10. This excessive ground current persisted for the duration of the event reports. As the data in the event report shows, these high currents can exist for an extended time after the transmission line fault clears.

Previous Delayed Voltage Recovery Sympathetic Tripping Solutions

To date, relay manufacturers and utility personnel have offered the following sympathetic trip solutions:

1. Increase the pickup thresholds of the phase and ground overcurrent protection elements.

This solution is simple, straight-forward, and effective. However, it desensitizes the protection to system faults. It is beneficial to temporarily raise overcurrent element pickup thresholds to avoid delayed voltage recovery sympathetic tripping. This increase in the time-overcurrent (TOC) element pickup need only be temporary and thus does not unnecessarily and permanently desensitize the feeder protection for forward (in-section) line faults.

2. Decrease fault clearing times to reduce the actual time that the motor loads are subjected to reduced voltage.

This approach is very good as it reduces the stall tendency of motors not in the immediate vicinity of the fault. Realizing the faster relay tripping times requires an investment in communications-assisted tripping schemes (relaying and communications equipment).

Faster fault clearing schemes for distribution lines are becoming more practical and cost-effective due to decreasing cost of digital communications equipment and channels [7].

3. Decrease the power system impedance to reduce line voltage drop.

When a system fault clears, the motor terminal voltage does not increase immediately. This is due to increased line-voltage drop from high load current drawn by stalled or stalling motors. Reduced motor terminal voltage increases the system voltage recovery time because it increases the time for motors to regain synchronous speed.

Decreasing the power line impedance from the source to the load decreases the line voltage drop (and increases the motor terminal voltage). The drawback of this solution is that it requires a large capital investment to increase conductor size and decrease transformer impedance.

4. Install undervoltage contactors for all motor loads.

This solution is perhaps the most effective as it removes stalled or stalling motor loads from the feeder. Removing these loads prevents the excessive motor load current flow following liberation of the initial fault. The downside of this solution is that it requires additional consumer cost and it is not directly controlled by the utility.

Additional General Guidelines for Mitigating Sympathetic Tripping

NPC has developed the following general guidelines to help mitigate the delayed voltage recovery (DVR) sympathetic tripping problem:

1. Lower individual feeder currents as much as is feasible.
2. Evenly divide the total load between feeders within a substation.
3. Balance each feeder load as much as possible to reduce prefault unbalance current. This prevents any standing unbalance current from possibly adding to the DVR caused unbalance current.

4. Use TOC characteristics that have a steep slope (more "inverse") to reduce the chance of sympathetic or cold load tripping problems.

RELAY-BASED SOLUTIONS TO PREVENT SYMPATHETIC TRIPPING

The following relay-based solutions prevent radial distribution feeder relays from tripping due to delayed voltage recovery sympathetic trip conditions. The solutions presented next differ in the method used to detect the conditions which precede the sympathetic trip.

The first method detects a simultaneous phase undervoltage without high current condition. The second method uses directional elements (32) for detection. After detection, the output of either detection logic uses higher set instantaneous overcurrent elements to torque control the TOC elements for a settable time.

Nevada Power Company System Protection Group's Present Methodology

Figure 17 shows the solution developed by NPC to solve the delayed voltage recovery sympathetic tripping problem described earlier. The logic shown in Figure 17 is the result of more than 20 years of customer outage investigation by the Nevada Power Company System Protection Group. These investigations were performed by both past and present field and engineering staff. This logic is now implemented in at least 50 distribution line terminals. Later we present field data which shows how effectively this logic worked for the recent NPC system faults described earlier in this paper.

The purpose of the logic shown in the dashed box of Figure 17 is to detect those conditions immediately preceding sympathetic tripping conditions: simultaneous low phase voltage and not high phase, negative- or zero-sequence current conditions. Recall from the previous examples that the high current condition did not occur until after the initial fault was cleared and the system voltage attempted to restore.

The remainder of the logic shown in Figure 17 also temporarily torque controls the TOC elements for the following three conditions:

1. When circuit demand encroaches upon the TOC element pickup thresholds.
2. The line breaker is just closed (Cold Load Pickup).
3. Upon receiving a local command.

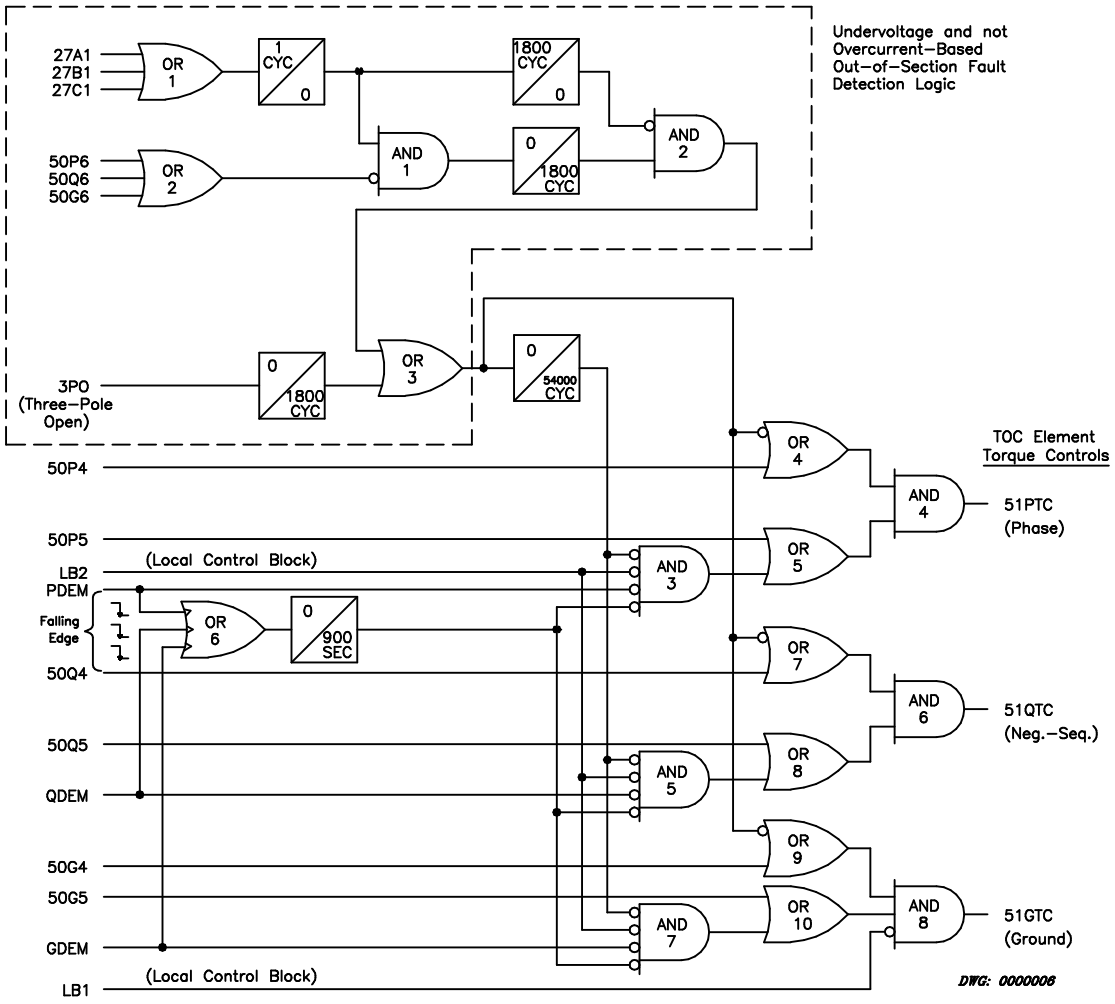

Figure 17: Nevada Power Company Sympathetic Trip Avoidance Logic

Methods of Altering TOC Element Timing

The follows list discusses ways to alter the TOC timing characteristics to achieve an increased time to trip:

1. Raise the TOC pickup threshold with a setting. This method moves the TOC characteristic to the right on multiples of current vs. time-to-trip plot. While secure, this method needlessly corrupts time coordination and increases the time to clear in-section faults.

2. Raise the TOC time dial setting to increase the trip time. Again, this method is secure but it corrupts time coordination and increases the time to clear in-section faults.

3. Control the TOC integration (timing) for current magnitudes below a new, higher set overcurrent element threshold. This method maintains the time to trip characteristic for higher current magnitudes and maintains coordination with downstream devices. Reference [8] describes additional means of achieving TOC timing modification for cold load pickup.

The logic shown in Figure 17 modifies the TOC characteristic by the method described in item 3 above. The phase TOC timing diagram shown in Figure 18 illustrates how using the higher set 50P4 and 50P5 phase overcurrent elements correctly modify the phase TOC timing characteristic: no operation for lower duty current magnitudes similar to those measured for delayed voltage recovery conditions, and no TOC timing alterations for higher duty faults.

Each TOC of the relay used by NPC has an individually programmable torque-control. For a TOC element to operate, the torque-control logic variable for that element must assert (become a logical 1). As an example, to enable the phase TOC element, the 51PTC logic variable shown in Figure 17 must assert. Once the delayed voltage recovery detection logic output asserts, the remaining logic blocks the phase TOC element from timing until higher set 50P4 or 50P5 overcurrent elements pick up.

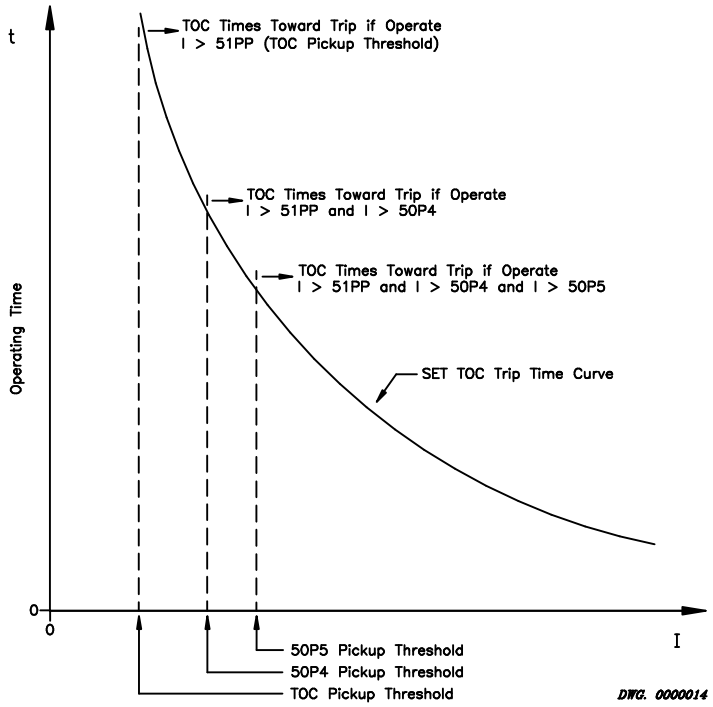

Figure 18: Torque-Controlling TOC Elements With High Set 50 Elements Does not Modify TOC Timing Characteristics for Higher Duty Faults (Phase Example)

Control Instead of Supervision Avoids Race Conditions and Maintains Coordination

Controlling when a TOC element begins timing is much different than simply supervising the TOC element output. The benefit of the control approach is that it reliably avoids contact race conditions. If, instead, we supervised the TOC element output with a higher set overcurrent (50) element, the TOC element could time-out but have its output blocked by the 50 element. If the 50 element then picked up momentarily for changing system conditions, the TOC element would instantaneously give an output. The effect of this type of supervision is that the TOC element undesirably behaves as an instantaneous element. Controlling the TOC timing with higher set 50 elements allows you to use the TOC element timing for coordination.

In-Section (Forward Direction) Distribution Line Fault

Let us next review how the logic in Figure 17 affects the phase TOC element torque control for two three-phase fault scenarios: a forward (in-section) line and an out-of-section fault.

For a forward three-phase line fault, all three phase-voltage magnitudes decrease while the magnitude of all three phase currents increase. These two conditions cause all three 27 elements and low-set phase overcurrent element (50P6) to pick up. Pickup of the 50P6 element blocks the AND 1 output. Because AND 1 is a logical 0, AND 2 is also a logical 0.

If the breaker has been closed (3PO is a logical 0) for 1800 cycles, the output of OR 3 is also a logical 0. This forces the output of OR 4 to a logical 1 (regardless of the status of the 50P4 element). Including 3PO in this logic automatically gives you cold load pickup logic functionality.

If the phase demand overcurrent element is not picked up (PDEM is a logical 0) and has not been asserted during the last 15 minutes, and if the local control block input is not asserted, the phase TOC torque control (51PTC) asserts without influence from the 50P5 overcurrent element. Because neither input to AND 4 is influenced by the pickup of 50P4 or 50P5, the phase TOC element timing matches the original minimum timing characteristics settings.

Out-of-Section (Reverse Direction) Fault

At the inception of a three-phase line fault elsewhere on the system, all three phase-voltage magnitudes decrease, yet the 50P6 element does not pick up. The combination of these two occurrences assert the AND 1, AND 2, and OR 3 outputs. Assertion of the OR 3 output blocks the output of AND 3. To assert the phase TOC torque control input during the next 1800 cycles (30 seconds), a phase current magnitude must exceed the higher set pickup thresholds of both the 50P4 and 50P5 overcurrent elements (again, see Figure 17).

After the 870 seconds following time-out of the 30 second time-delayed dropout timer, any phase current must exceed the 50P5 threshold to enable the 51P element.

The effect of using two 50 elements with different settings is to “stair-step” the phase TOC torque control. This stepping-down of the TOC torque control minimum current threshold follows the expected decrease in line current as the motor load regains synchronous speed (recall Figure 3).

THE FAULT INDUCED LOAD UNBALANCE SYMPATHETIC TRIPPING PROBLEM

Figure 19 shows the system single-line diagram and sequence connection diagrams for a single-line-ground (SLG) fault on a radial line. For the fault shown, Breaker X should clear the fault while Recloser Y remains closed. Tripping Recloser Y for the fault shown results in confusing targets for field personnel (which could cause unnecessary line patrolling) and needless recloser contact wear.

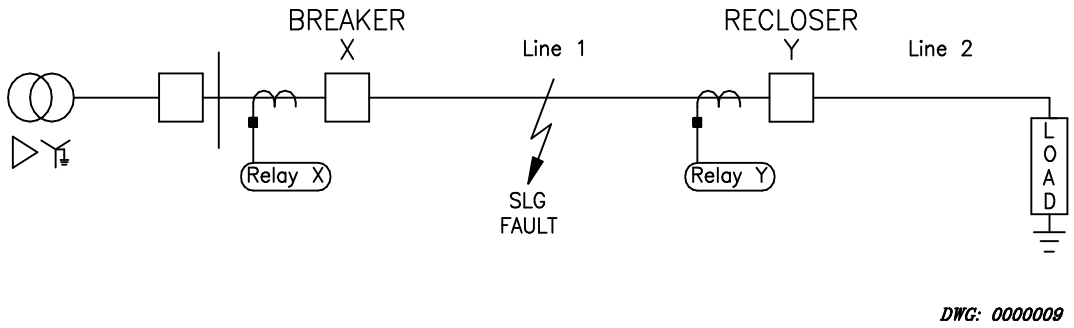

Figure 19: System Single-Line Showing a Radial Line With a Ground Fault

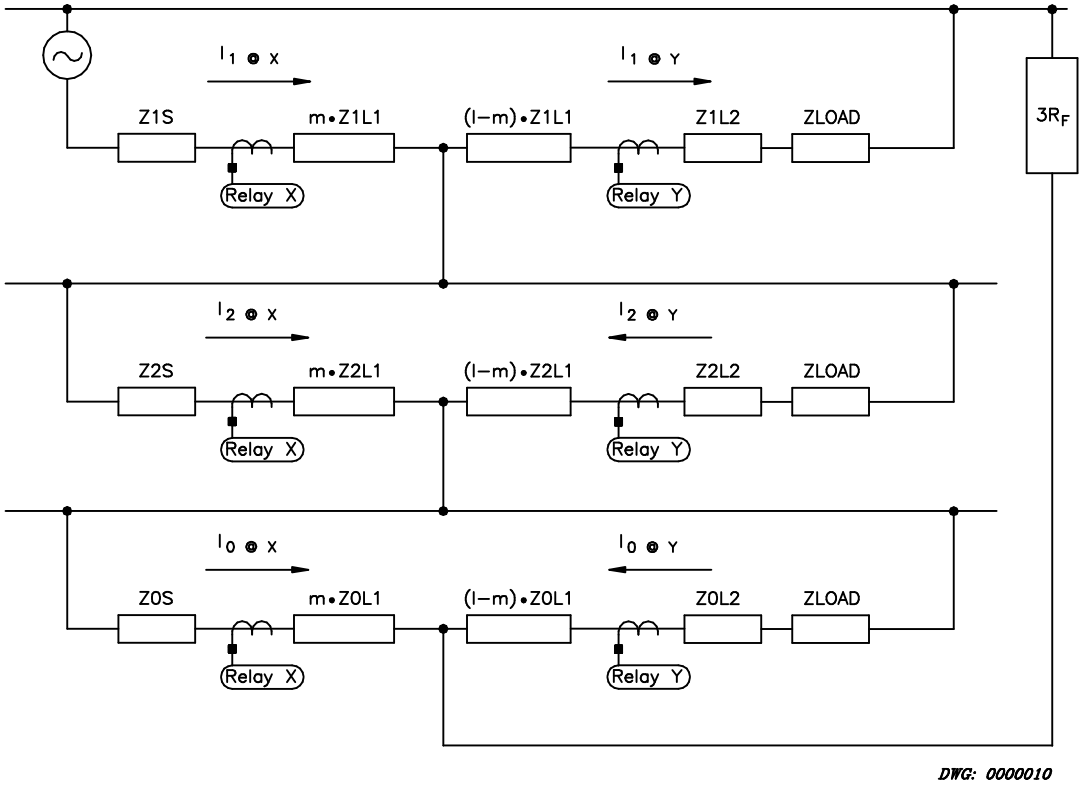

I_1 ° Positive-Sequence Current I_2 ° Negative-Sequence Current I_0 ° Zero-Sequence Current

Figure 20: Sequence Connection Diagram of Single-Line-Ground Fault on a Radial Feeder With End of Line Grounded-Wye Load

In the example system shown in Figure 19, load is connected phase-ground at the end of the feeder. With this load connection, the same value of Z_{LOAD} is included in all three sequence networks of Figure 20. If the load is instead connected phase-phase, Z_{LOAD} is an infinite impedance in the zero-sequence network.

From Figure 20, notice that Z_{LOAD} redistributes the total zero-sequence ($3I_0$) and negative-sequence ($3I_2$) currents. This current redistribution affects the sensitivity of Relay X. Z_{LOAD} decreases the $|3I_0|$ and $|3I_2|$ current measurable by Relay X. This fact encourages us to lower

the ground overcurrent element pickup threshold for Relay X to maintain ground-fault sensitivity.

The presence of Z_{LOAD} in the negative- and zero-sequence networks permits Relay Y to measure $3I_0$ and $3I_2$ currents for a reverse fault. This fact might motivate us to increase the ground overcurrent element pickup thresholds for Relay Y to desensitize the protection for reverse faults. However, doing this undesirably desensitizes Relay Y protection for forward ground faults and complicates coordination with Relay X.

If the nondirectional ground or negative-sequence overcurrent element pickup thresholds for Relay Y are low set, either of these elements could trip undesirably for the reverse fault shown. Whether or not these elements operate depends upon the fault placement and load impedance magnitude.

For ungrounded feeder loads, Z_{LOAD} does not desensitize the zero-sequence ground overcurrent protection at Relay X. In such applications, the risk of tripping Relay Y for the fault shown in Figure 19 is minimal because the relay does not sense zero-sequence current for reverse faults involving ground.

DIRECTIONAL CONTROL PERMITS LOWER AND SECURE PICKUP THRESHOLDS

To maintain ground-fault sensitivity, we need to lower the pickup of the ground overcurrent elements at Relay X. This allows Relay X to maintain the same degree of ground fault resistance coverage as when the load is not connected. However, lowering the overcurrent pickup settings of Relay X may require lowering ground overcurrent pickup settings at Relay Y. This makes Relay Y more susceptible to operating for reverse faults.

Sensitive ground overcurrent thresholds at Relay Y require directional control to maintain the same degree of security as higher pickup thresholds. These overcurrent thresholds must be set above normal system unbalance unless the ground directional element includes security logic to account for the maximum expected load unbalance [2],[6].

Fault Induced Sympathetic Tripping Example

Let us use the following example to see how directional control permits secure, low set ground overcurrent element thresholds for Relay Y. For the example radial system shown in Figure 19, assume the following secondary system impedance values:

Positive-Sequence Source, Line Impedances: $Z_{1S} = Z_{1L1} = Z_{1L2} = 1\ \Omega\ \angle 90°$

Zero-Sequence Source and Line Impedances: $Z_{0S} = Z_{0L1} = Z_{0L2} = 3\ \Omega\ \angle 90°$

Per-Phase Load Impedance: $Z_{LOAD} = 20\ \Omega\ \angle\ 0°$

Using symmetrical component analysis, we can easily calculate the negative- and zero-sequence current values presented to Relays X and Y. Table 1 summarizes the results of these calculations for the Line 1 fault placed at m = 0.5; where m = per-unit line length (the driving source voltage for this example is 66.4 V secondary).

Table 1: Current Magnitudes for the A-Phase-Ground Fault Shown in Figure 19

Measurement Location	I_{PHASE} (PREFAULT)	I_{PHASE} (FAULT)	I_2 (FAULT)	I_0 (FAULT)	V_2 (FAULT)	V_0 (FAULT)
Relay X	3.3A ∠-8.5°	27.32A ∠-85.5°	9.11A ∠-90.1°	8.59A ∠-97.4°	---	---
Relay Y	3.3A ∠-8.5°	0.29A ∠-12.8°	0.68A ∠175.7°	1.89A ∠159.9°	13.67V ∠-180°	38.66V ∠173°

From Table 1, a nondirectional ground overcurrent element at Relay Y with a pickup threshold less than 5.67 A secondary (operate current of $3I_0$) operates for the reverse fault shown in Figure 19.

Directional Elements Prevent Recloser Sympathetic Tripping

From Table 1, notice that the direction of negative- and zero-sequence current is into the bus at Relay Y. This is the same current flow direction as that of a reverse fault involving ground. Because our example system is radial, any reverse fault declaration by the ground directional element should temporarily raise the operate threshold of the ground time-overcurrent element.

Directional Element Approach For Detecting Sympathetic Trip Conditions

Relays applied to a radial distribution feeder measure negative-sequence current flowing into the bus for out-of-section unbalanced faults. This current flow direction is the same as that for a reverse fault. Thus, we can use unbalanced fault directional elements and other logic to detect the conditions which proceed a sympathetic trip.

Detecting Out-of-Section Unbalanced Faults

For a radial distribution feeder, any fault which appears reverse to a directional element must be out-of-section. Detect this reverse fault condition using a combination of unbalanced fault directional elements.

Use a negative-sequence directional element for reverse fault declarations. This directional element can sense reverse unbalance faults whether the feeder load is connected phase-ground, phase-phase, or if there is a delta-wye connected power transformer between an out-of-section, single-line-ground fault and the relay location.

To increase the sensitivity of the directional element for detecting external faults (where ground fault current is presented to the relay), the complete unbalanced fault directional element makeup also includes a zero-sequence directional element. This element is active for unbalanced faults where the zero-sequence current magnitude is some multiple (greater than one) of the negative-sequence current magnitude [6].

As we saw in the data plots earlier, the feeder relays measure unbalance current both during and after the reverse fault. The magnitude of this unbalance current diminishes with time as the motors either regain synchronous speed or trip by their own thermal overload protective devices. This tells us that the protection must “ride-through” this unbalanced time period. Do this by temporarily increasing the TOC element pickups. We can mimic the reduction in feeder current

with time as a series of decreasing threshold steps where the pickup threshold of each step is less than the previous step. The final step is the set pickup of the TOC element. This is the same approach as that described in the NPC developed logic.

The reverse fault declaration output from this directional element is used as one of the inputs to a programmable timer. This time delay duration is settable via a general purpose time-delayed pickup (TDPU), time-delayed dropout (TDDO) timer settings. The output of this timer is then used in the logic which temporarily raises the pickup of the TOC elements.

Unbalanced Fault Directional Element (patent pending)

A modified negative-sequence directional element (32Q) detects all out-of-section unbalanced faults. The modification is that the directional element automatically switches between two directional measurement algorithms. The decision of which algorithm to use is based upon the measured angle difference between V_{A2} and I_{A2}: $\angle Z_2$. The unbalanced fault directional element uses the algorithm described by Equation 1 if $\angle Z_2$ is greater than 30°. When $\angle Z_2$ is less than 30°, the relay uses Equation 2 for directional calculations.

$$\mathrm{Re}\left[V_{A2} \bullet \left(I_{A2} \bullet 1\angle Z_{1L}\right)^{*}\right] / \left|I_{A2}\right|^{2} \qquad \text{Equation 1}$$

$$\mathrm{Re}\left[V_{A2} \bullet \left(I_{A2}\right)^{*}\right] / \left|I_{A2}\right|^{2} \qquad \text{Equation 2}$$

where

- Re ≡ Real component
- V_{A2} ≡ Negative-sequence voltage referenced to A-phase
- I_{A2} ≡ Negative-sequence current referenced to A-phase
- Z_{1L} ≡ Positive-sequence replica line impedance
- * ≡ Complex conjugate

Equations 1 and 2 differ in that Equation 1 includes a phase angle shift of I_{A2}. The rationale for this difference is best illustrated by reviewing the phasors shown in Figure 21. These phasors represent the prefault and fault voltage and current phasors measured by a protective relay on a radial, nonfaulted feeder for an A-phase fault on an adjacent radial feeder. For the balanced prefault load conditions, the angle difference between $V_{a\ pre}$ and $I_{a\ pre}$ is the feeder load angle. Notice that $I_{a\ pre}$ lags $V_{a\ pre}$ slightly. This indicates that the feeder is serving a slightly inductive load.

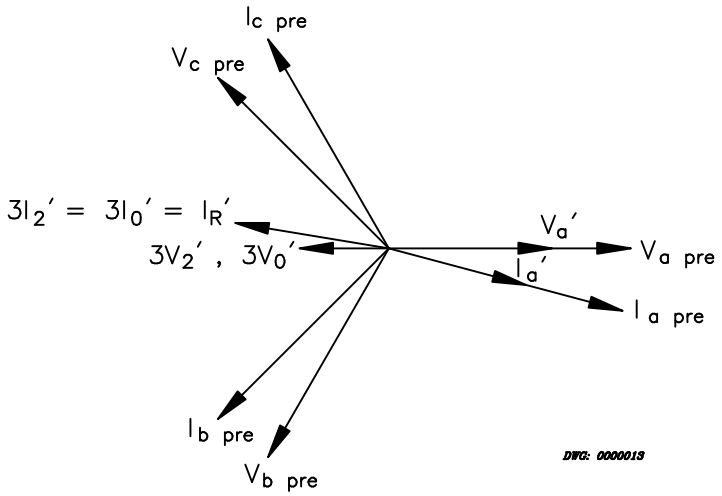

$V_{a,b,c\ pre}$ ≡ Prefault A-, B-, and C-Phase Voltages
$I_{a,b,c\ pre}$ ≡ Prefault A-, B-, and C-Phase Currents
V_A' ≡ A-Phase Fault Voltage
I_A' ≡ A-Phase Fault Current
$3I_0$' ≡ Ground Current Due to the A-Phase Fault
$3I_2$' ≡ Negative-Sequence Current Due to the A-Phase Fault
$3V_0$' ≡ Zero-Sequence Voltage Due to the A-Phase Fault
$3V_2$' ≡ Negative-Sequence Voltage Due to the A-Phase Fault

Figure 21: Phase and Sequence Phasors for Prefault and Out-of-Section Ground Fault While Serving a Low-Angle Load

From Figure 21, notice that the angular difference between $3V_2$' and $3I_2$' is small (less than 30°). Without adjusting the angle of $3I_2$' by the replica line angle, the directional calculation of $\text{Re}[V_2 \cdot (I_2')^*]$ is desirably large and positive (positive indicates a reverse fault). Adjusting $3I_2$' by the feeder line angle for the sequence quantities given in Figure 21 (as would Equation 1) decreases the magnitude of the directional calculation making directional decisions difficult.

Typical power sources are very inductive and feeder loads are more resistive. As the type of loads (highly inductive or resistive) can vary throughout the day, a complete directional element must use the two different algorithms described by Equations 1 and 2. If the feeder load impedance angle is always high, the algorithm shown in Equation 1 is the appropriate choice for all directional declarations. Having both algorithms available for directional calculations makes this directional element logic applicable to most feeder circuits with both inductive and resistive loads that can be switched on or off at any time.

Out-of-Section Balanced Fault Detection Logic (patent pending)

We cannot rely upon negative- or zero-sequence polarized directional elements to detect balanced out-of-section faults. Figure 2 showed the sequence connection diagram for a fault on an adjacent feeder. Notice in Figure 2 that the direction of I_1 does not change direction during the out-of-section fault. This observation shows us that a phase directional element on the nonfaulted feeder cannot make a reverse fault declaration for a fault on an adjacent or source power line. When applied to radial feeders, phase directional element decisions must either be defeated, overridden, or not used to avoid conflicting fault direction declarations to the torque controlled protective overcurrent elements.

To declare an out-of-section three-phase fault condition, we instead detect a simultaneous decrease in phase voltage and current for all three phases. The following are balanced out-of-section fault detection criteria: the magnitude of each phase voltage decreases by 10% and the decrease in each phase current is more than 0.25 A (as compared to the previous cycle). If the relay detects these decreases on all three phases simultaneously, the relay asserts the logic point labeled LD32P. Notice that LD32P is completely independent from the other directional logic to avoid directional decision conflicts discussed above.

Directional Element Sympathetic Trip Avoidance Logic

The complete logic required to avoid sympathetic tripping using the modified unbalanced fault directional elements and LD32P logic is very similar to the NPC logic shown earlier. The only difference between the logic shown in the dashed box of Figure 17 and that shown next is the out-of-section fault detection logic.

Figure 22 illustrates the logic necessary to replace that logic shown inside the dashed box in Figure 17. Any out-of-section fault asserts either the 32GR or LD3P logic points.

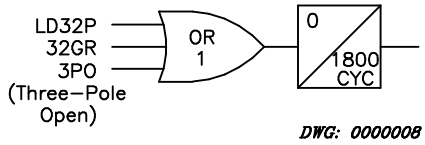

Figure 22: Directional Element Based Out-of-Section Fault Detection Logic

A significant advantage to this approach is it does not require user settings. This is a significant benefit given that the threshold settings for the phase undervoltage elements (27A1, 27B1, 27C1) and overcurrent fault detector elements (50P6, 50Q6, 50G6) may be difficult to determine for all feeder switching configurations and loading. In the case of NPC's system, the 12.47 kV feeder fault duties, switching configurations, and loading are well known.

The same sympathetic trip avoidance logic shown in Figure 22 is also very applicable to applications at risk of tripping for fault-induced sympathetic tripping.

Directional Element Logic Performance for Out-of-Section 69 kV Fault

The directional element logic described above is not installed in the relays for Feeders 1210 and 1215. To determine how this new directional element sympathetic trip avoidance logic would have performed for the NPC fault described earlier, we used the data retrieved from the feeder relays as input to a computer simulation. Let us next examine how this logic would have performed for Feeder 1215 during and after the 69 kV fault.

We know that the initial 69 kV transmission line fault was unbalanced. For this fault, we expect the feeder relays to use the unbalanced directional element (32GR) to declare the fault direction as reverse.

From the Feeder 1215 relay event report data, first calculate $\angle Z_2$ and determine which algorithm the 32Q element would use for this fault. Figure 23 shows the calculated $\angle Z_2$ for the entire event report. Please note that the angle data shown in Figure 23 prior to the 69 kV fault inception is not reliable because the magnitude of the negative-sequence quantities is very small. For this very reason, the 32Q element calculations are disabled until the relay measures $3I_2$ greater than a minimum set threshold.

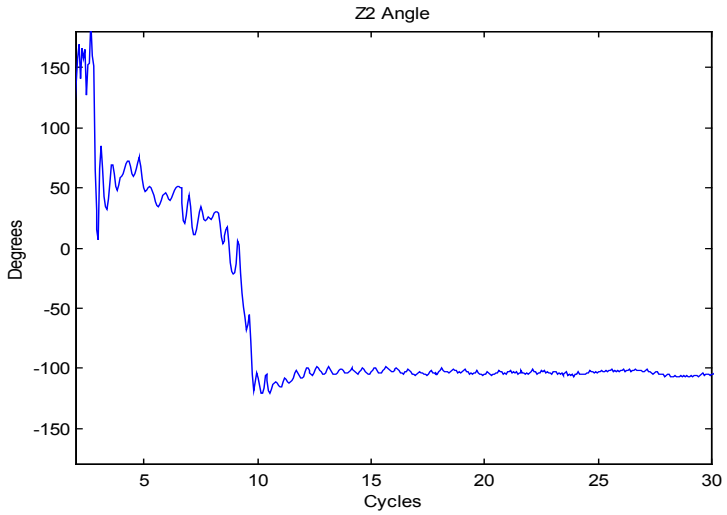

Figure 23: Angular Difference Between V_{A2} and I_{A2} Measured by Feeder 1215 Relay During and After the NPC 69 kV Ground Fault

From Figure 23, notice that after fault inception the $\angle Z_2$ is initially greater than 30° and remains so until approximately six cycles. Using this angle information, the unbalanced fault directional element uses the negative-sequence impedance calculation with line angle compensation until after Cycle 6. After six cycles, the 32Q element uses the noncompensated directional element algorithm.

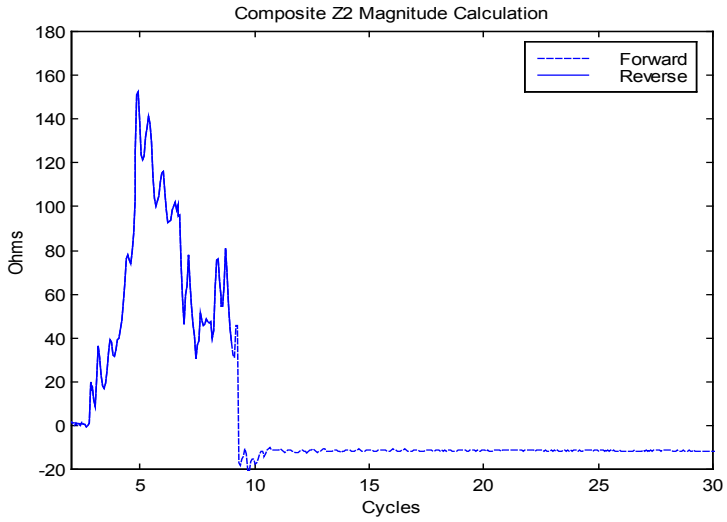

Figure 24: Composite 32Q Directional Element Calculation Results for Feeder 1215 Relay During and After the NPC 69 kV Ground Fault

Figure 24 shows the unbalanced fault directional element calculation for this fault. The relay should declare a reverse fault when the calculated negative-sequence impedance is greater than one-half of the replica line impedance plus 0.1 Ω. In this case, the replica line impedance is 2 Ω secondary. From this figure we can see that the angle-compensated directional element correctly declares the 69 kV fault as reverse because the calculated impedance is greater than 1.1 Ω secondary after fault inception. (From [6], the reverse directional threshold is automatically set at one-half of the replica line impedance plus 0.1 Ω). At approximately 6 cycles, where the unbalanced fault directional element uses the algorithm described by Equation 2, the 32Q element continues to declare the out-of-section fault as reverse but has a larger output result to compare against the reverse setting threshold. Near Cycle 10, where the high-voltage fault evolved, the 32Q element operation is blocked by negative-sequence overcurrent supervision logic.

New Sympathetic Trip Logic Performance Comparison

How do these new sympathetic logic schemes perform for actual out-of-section faults? Let us next compare the performance of that logic shown in the dashed box in Figure 17 (undervoltage and not overcurrent) and the directional scheme logic of Figure 22 for Feeder 1215 during the 69 kV fault described earlier.

The last frame of Figure 25 shows a timing comparison of these two logics. As expected, both logic schemes correctly asserted (shown as a transition from a logical 0 to a logical 1 in the last frame of Figure 25). Also notice that the unbalanced fault directional element logic detects the out-of-section fault faster than does the undervoltage-based logic. This time difference is due to two things: 1) the undervoltage-based scheme requires a 27 element pickup delay to avoid false logic assertions during voltage transients and to allow some time for the overcurrent elements to pick up, and 2) undervoltage elements set to $0.85 \bullet V_{NOM}$ are typically slower than directional elements. After careful review of the data, NPC engineers realized that the one-cycle pickup delay for the 27 elements needs to be decreased to 0.5 cycles (perhaps even 0.25 cycles).

Comparing the undervoltage and not overcurrent logic (Figure 17) and the directional element-based sympathetic trip avoidance logic (Figure 22), we see that the latter is much simpler. In addition to being simpler, the directional element logic actually eliminates setting requirements. Table 2 lists a simple comparison of these two sympathetic trip approaches.

Table 2: Contrasting Sympathetic Trip Logic of Figure 17 and Figure 22

	Figure 17	Figure 22
# AND gates	2	0
# OR gates	3	1
# Timers*	3	0
# Settings	7	0

* Not including 3PO driven timer.

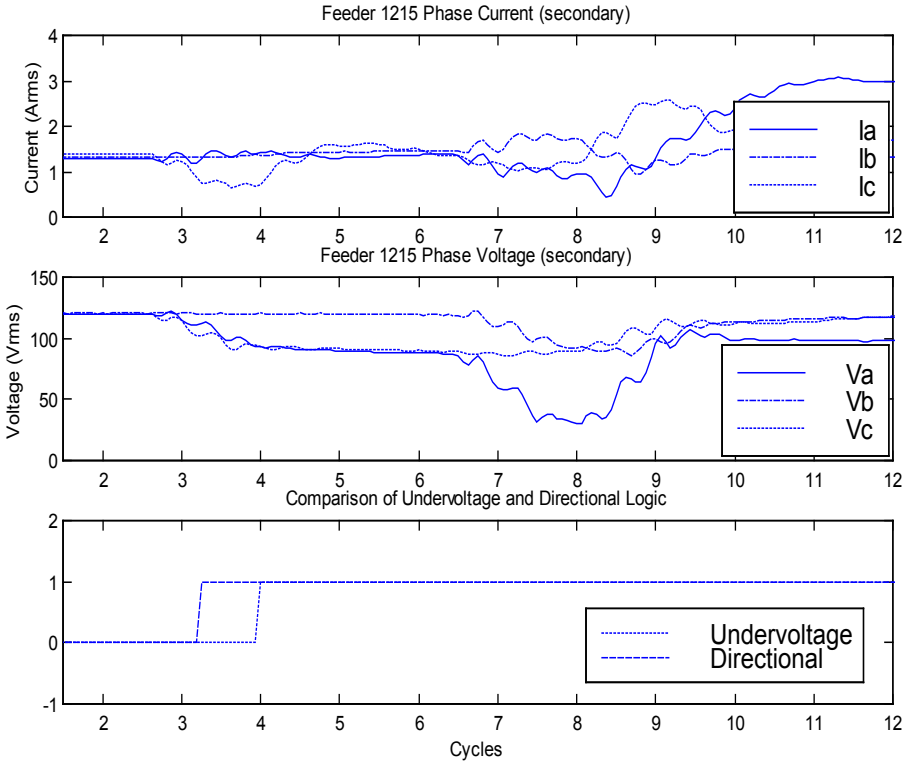

Figure 25: Performance Comparison of the Two New Sympathetic Trip Logics

SUMMARY

Important points presented in this paper include

1. Load impedances effect the sensitivity of ground overcurrent elements. Lowering the pickup thresholds of the ground overcurrent elements restores fault detection sensitivity.

2. These same loads allow downstream relays to measure fault current for reverse ground faults. Because these relays measure residual current for reverse ground faults, they are at risk for sympathetic tripping.

3. Directional elements give sympathetic tripping security for radial feeders. Torque-controlling overcurrent elements with directional elements solve fault-induced sympathetic tripping problems identified in 1 and 2, above.

4. Single-phase, low-inertia motor loads stall during the depressed voltage conditions for a fault. These motor stalls cause delayed voltage recovery (DVR) problems for power systems. The DVR problem for feeder protection manifests itself as large phase and sequence currents following fault clearance. Because these large currents can be many times the pickup threshold of the time-overcurrent elements used to protect the feeder, these relays are at risk for sympathetic tripping.

5. We present two viable methods for detecting the out-of-section faults which precede the high current conditions for a DVR condition: 1) phase undervoltage and not overcurrent, and 2) directional elements for unbalanced faults and DV/DI for balanced faults.

6. For the two sympathetic tripping logic schemes presented, the directional element-based methodology requires fewer settings and gives a quicker out-of-section fault declaration.

REFERENCES

[1] E. O. Schweitzer III and J. Roberts, "Distance Element Design," Proceedings of the 19th Annual Western Protective Relay Conference, Spokane, WA, October 1992.

[2] E. O. Schweitzer III, J. Roberts, E. Poggi, R. Arora, "Limits to the Sensitivity of Ground Directional and Distance Protection," Proceedings of the 19th Annual Western Protective Relay Conference, Spokane, WA, October 1992.

[3] B. R. Williams, W. R. Schmus, and D. C. Dawson, "Transmission Voltage Recovery Delayed by Stalled Air Conditioner Compressors," IEEE Transactions on Power Systems, Vol. 7, No. 3, August 1992.

[4] D. Jackson, "Sympathetic Tripping on Distribution Feeders," Proceedings of the 46th Annual Conference for Protective Relay Engineers, Texas A&M University, College Station, TX, April 1993.

[5] R. E. Owen, "Solutions to Sympathetic Tripping of Distribution Feeders," Rocky Mountain Electric League, Colorado Springs, CO, May 1977.

[6] A. Guzmán, J. Roberts, D. Hou, "New Ground Directional Element Operates Reliably for Changing System Conditions," Proceedings of the 23rd Annual Western Protective Relay Conference, Spokane, WA, October 1996.

[7] K. Behrendt, "Relay-to-Relay Digital Communication for Line Protection and Control," Proceedings of the 23rd Annual Western Protective Relay Conference, Spokane, WA, October 1996.

[8] O. Mirza, "A Novel Approach to Handle the Cold Load Pickup Problem," Proceedings of the 22nd Annual Western Protective Relay Conference, Spokane, WA, October 1995.

BIOGRAPHY

Jeff Roberts received his BSEE from Washington State University in 1985. He worked for Pacific Gas and Electric as a Relay Protection Engineer for over three years. In 1988, he joined Schweitzer Engineering Laboratories, Inc. as an Application Engineer. He now serves as the Research Engineering Manager.

He has written many papers in the areas of distance element design, sensitivity of distance and directional elements, directional element design, and analysis of event report data.

Mr. Roberts holds multiple patents and has other patents pending. He is also a member of IEEE.

Terrance L. Stulo received his BSEE from University of Wisconsin, Madison in 1983. He worked as a protection engineer for several Midwest utilities and a federal power marketing agency. Presently, he is Team Leader for the System Protection Group at Nevada Power Company. He holds a PE in the state of Wisconsin.

Andres Reyes received his BSEE and his BSME from the Autonomous University of Santo Domingo in 1982. He worked in a manufacturing industry from 1982 through 1990. In 1990, he joined Nevada Power Company where his last position was System Protection Engineer until May of 1997. Presently, he is an Application Engineer for Omicron Electronics Corp. USA.

APPENDIX A

ZCALC.MCD S. E. Zocholl 12/20/92

Calculates motor impedance as a function of slip from motor nameplate data.

FLA := 271 Rated current

RHP := 1200 Rated horse power

LRA := 1626 Locked rotor current

QLR := .8 Locked rotor torque

FLW := 1783 Rated full load speed

SynW := 1800 Synchronous speed

$I_L := \frac{LRA}{FLA}$ Per unit locked rotor torque

$rad := \frac{p}{180}$

$j := \sqrt{-1}$

$I_L := 6$

$R_0 := \frac{SynW - FLW}{SynW}$ Rotor resistance at rated speed

$R_1 := \frac{QLR}{I_L^2}$ Rotor resistance at lock rotor

$R_3 := \frac{R_0}{5}$ Stator resistance

$R := R_1 + R_3$ Total motor resistance

$Z := \frac{1}{I_L}$ Total motor impedance

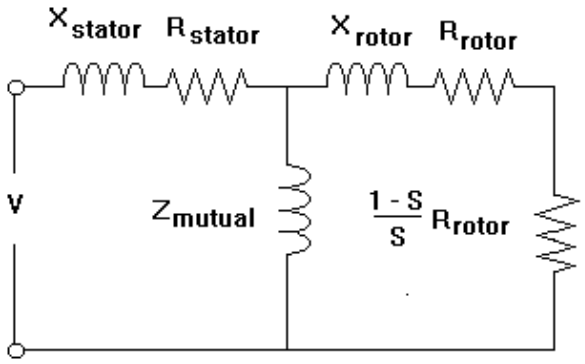

$X := \sqrt{Z^2 - R^2}$ Total reactance

$X_1 := \frac{X}{2}$ Locked rotor reactance Nema Std for QLR <1 (for QLR >1 use 2/3)

$X_3 := X + X_1$ Stator reactance

$X_0 := \frac{\tan(12.75 \cdot rad)}{1 + R_0 + R_3} - X_3$ Rotor reactance at rated speed

$X_m := 5$ Motor mutual impedance (assumed value)

Motor Impedance Calculation

i := 0..14 Index for number of slip calculations

$\omega_i := i \cdot .07$ Speed $s_i := 1 - w_i$ Slip

$$Rrotor_i := \frac{R_1 - R_0}{1 - R_0} \cdot (1 - \omega_i) + \frac{(R_0 - R_1 \cdot R_0)}{1 - R_0}$$ Rotor resistance

$$Xrotor_i := \frac{X_1 - X_0}{1 - R_0} \cdot (1 - \omega_i) + \frac{(X_0 - X_1 \cdot R_0)}{1 - R_0}$$ Rotor reactance

$$Z_{stator} := R_3 + j \cdot X_3 \qquad Z_{rotor_i} := \frac{Rrotor_i}{1 - \omega_i} + j \cdot Xrotor_i \qquad Z_{mutual} := j \cdot X_m$$

$$Z_{motor_i} := Z_{stator} + \frac{Z_{rotor_i} \cdot Z_{mutual}}{Z_{rotor_i} + Z_{mutual}}$$ Impedance at terminals

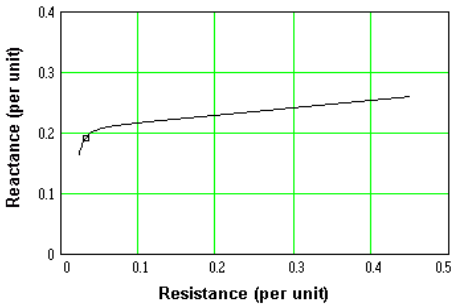

i	w_i	s_i	$\lvert Z_{motor_i} \rvert$	$\frac{\arg(Z_{motor_i})}{rad}$	Z_{motor_i}
0	0	1	0.165	81.865	0.023 + 0.164i
1	0.07	0.93	0.169	81.843	0.024 + 0.168i
2	0.14	0.86	0.173	81.785	0.025 + 0.172i
3	0.21	0.79	0.178	81.687	0.026 + 0.176i
4	0.28	0.72	0.182	81.538	0.027 + 0.18i
5	0.35	0.65	0.186	81.324	0.028 + 0.184i
6	0.42	0.58	0.19	81.024	0.03 + 0.188i
7	0.49	0.51	0.194	80.607	0.032 + 0.192i
8	0.56	0.44	0.199	80.02	0.034 + 0.196i
9	0.63	0.37	0.203	79.17	0.038 + 0.2i
10	0.7	0.3	0.208	77.885	0.044 + 0.204i
11	0.77	0.23	0.215	75.786	0.053 + 0.208i
12	0.84	0.16	0.223	71.895	0.069 + 0.212i
13	0.91	0.09	0.245	62.746	0.112 + 0.218i
14	0.98	0.02	0.521	30.062	0.451 + 0.261i